Implementation of transformed lenses in bed of nails reducing refractive index maximum value and sub-unity regions

Daniel R. Prado,[1,*] Andrey V. Osipov,[2,4] and Oscar Quevedo-Teruel[3,5]

[1]*Department of Electrical Engineering, Group of Signal Theory and Communications, Universidad de Oviedo, Gijón, Spain*

[2]*Research Institute of Radio Engineering and Telecommunications, Saint Petersburg Electrotechnical University, Saint Petersburg, Russia*

[3]*School of Electrical Engineering, KTH Royal Institute of Technology, Stockholm, Sweden*

[4]*e-mail: andrew.v.osipov@gmail.com*

[5]*e-mail: oscarqt@kth.se*

**Corresponding author: drprado@tsc.uniovi.es*

Received December 17, 2014; revised January 29, 2015; accepted January 30, 2015;
posted February 2, 2015 (Doc. ID 230721); published March 4, 2015

Transformation optics with quasi-conformal mapping is applied to design a Generalized Maxwell Fish-eye Lens (GMFEL) which can be used as a power splitter. The flattened focal line obtained as a result of the transformation allows the lens to adapt to planar antenna feeding systems. Moreover, sub-unity refraction index regions are reduced because of the space compression effect of the transformation, reducing the negative impact of removing those regions when implementing the lens. A technique to reduce the maximum value of the refractive index is presented to compensate for its increase because of the transformation. Finally, the lens is implemented with the bed of nails technology, employing a commercial dielectric slab to improve the range of the effective refractive index. The lens was simulated with a 3D full-wave simulator to validate the design, obtaining an original and feasible power splitter based on a dielectric lens.

OCIS codes: (080.3620) Lens system design; (080.3630) Lenses; (160.3918) Metamaterials; (220.3620) Lens system design; (220.3630) Lenses.

http://dx.doi.org/10.1364/OL.40.000926

Since the introduction of transformation optics by the pioneering works of Leonhardt [1] and Pendry *et al.* [2] for cloaking, its development and number of applications have significantly grown [3]. This technique is based on the form invariance of Maxwell equations under coordinate transformations and allows the design of alternatives to traditional devices such as wave collimators [4,5], flat lenses [6,7], beam benders [5], shifters, splitters [8], waveguides [9], and beam expanders/compressors [10], as well as new classes of devices such as electromagnetic wormholes, virtual magnetic monopoles [11], and cloaks [12,13].

In this Letter, we propose the use of quasi-conformal transformation optics (QCTO) [14] to design a Generalized Maxwell Fish-eye Lens (GMFEL) [15] which can be employed as a power splitter with a flattened focal line to adapt it to planar antenna feeding systems. Because of the space compression of the transformation, the sub-unity refractive index regions are reduced, thus minimizing the negative effects in performance caused by the removal of such regions. QCTO allows minimization of the material anisotropy [14,16] which can be approximated by an isotropic dielectric, making the lens easier to manufacture.

Because of the nature of the employed transformation, the new refractive index distribution has a large maximum value, which might be difficult to manufacture. Thus, a technique to reduce such value is presented at the expense of reducing slightly the flattened focal line. This technique can be combined with approximations to further reduce the maximum value of the refractive index while preserving the lens performance (for instance, artificially restricting the range of the refractive index after the transformation).

Finally, the transformed lens is implemented with a modified bed of nails in parallel plate technology. A dielectric slab below the top plate is employed to increase the range of the refractive index as a function of the height of the nails. The final lens was simulated with a 3D full-wave simulator, proving its feasibility to work as a novel power splitter.

The refractive index profile of the GMFEL is [15]

$$n(r) = \sqrt{\varepsilon_r} = \frac{2(r/a)^{1/M-1}}{1+(r/a)^{2/M}}, \tag{1}$$

where a is the radius of the lens and $M > 0$ is a parameter that determines the behavior of the lens. For M odd, the lens generates an image of the source in the opposite side. For M even, it behaves as a monopole. For non-integer values of M, the GMFEL works as a power splitter. The original circular lens is mapped with QCTO as shown in Fig. 1, where the original and transformed spaces are shown. In addition, a parameter y_0 is introduced to tune the distribution of the resulting refractive index after the transformation. This parameter represents a shift in the lens placement so that for $y_0 = 0$ half the lens is flattened and for $y_0 = 1$ the original shape is preserved.

A rigorous implementation of transformation optics leads to highly anisotropic materials [17] which are hard to manufacture and present high losses and reduced bandwidth [16]. To overcome these limitations, the approximate transformation described by Li and Pendry [14] is used here. Let (x, y) be the coordinates in the original space and (u, v) in the transformed one. Then, the Jacobian matrix is defined as

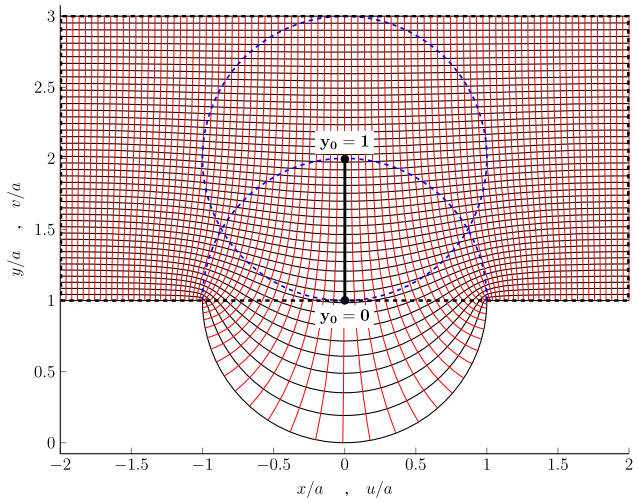

Fig. 1. Original space with quasi-conformal mapping (black and red solid lines, (x, y) coordinates), lens placement (blue dashed lines) and contour of transformed space (black dashed line, (u, v) coordinates). The transformed space is mapped into a regular grid with the same number of cells in each dimension as the original space.

$$J = \begin{pmatrix} \frac{\partial x}{\partial u} & \frac{\partial x}{\partial v} \\ \frac{\partial y}{\partial u} & \frac{\partial y}{\partial v} \end{pmatrix}, \tag{2}$$

and the relative permittivity in the transformed space is calculated as

$$\varepsilon_r' = \sqrt{\det(J^T J)}\varepsilon_r, \tag{3}$$

where ε_r is the relative permitivity in the original space, which is mapped using quasi-conformal mapping as shown in Fig. 1. As an advantage of this implementation, the transformed space will have $\mu_r' \approx 1$ and the anisotropy will be minimized [14]. The transformed space is defined as the rectangle shown in Fig. 1 with a black dashed line (as a result of flattening in the original space) and is discretized with a uniform grid with the same number of cells in both dimensions as the original space.

Developing the determinant in Eq. (3) will yield the scale factor because of the transformation as

$$\sqrt{\det(J^T J)} = \left(\frac{\partial x}{\partial u}\frac{\partial y}{\partial v} - \frac{\partial x}{\partial v}\frac{\partial y}{\partial u}\right). \tag{4}$$

One effect of the transformation is the space compression. This can be beneficial for lens design since it allows reducing of the sub-unity refractive index regions. The original GMFEL presents these areas for $M \in (0, 1)$. When implementing them, the resulting materials tend to have reduced bandwidth because they are inherently dispersive [16]. The transformation reduces these regions because of the space compression effect, as shown in Fig. 2. There, contour L bounds the sub-unity region in the original lens and is transformed into contour L', which is smaller in area. However, in the transformed lens, contour C is the one that bounds the sub-unity region, which is smaller than L'. This effect is stronger for values of y_0 closer to 0.

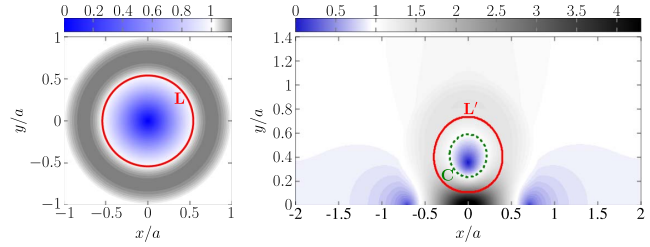

Fig. 2. Effect of the space compression on the sub-unity refraction index regions. Such regions are larger in the original GMFEL (left, bound by L) than in the transformed one (right, bound by C). Example for $M = 0.5$ and $y_0 = 0$.

For the exemplary case at hand, when flattening half the lens, the maximum value of n will reach its maximum (not considering flattening more than half the lens). This case corresponds to $y_0 = 0$, and max $n \approx 4.5$, as shown in Fig. 3 for three different lenses. When $y_0 = 1$, there is no flattening; the transformation is the identity and thus the lens shape is preserved. For other values $y_0 \in (0, 1)$, less than half of the lens is flattened. By shifting the lens slightly, the refractive index rapidly decreases. For a shift of $y_0 = 0.25$, which corresponds to a quarter of the radius of the original lens, max n decreases from 4.5 to less than 3.25. As the lens is shifted more, max n decreases at a slower pace for $M = 1$ and $M = 0.8$, and the flattened focal line is also reduced until the limit case of $y_0 = 1$ is reached. Another effect of shifting the lens is the reduction of the sub-unity refractive index regions on the sides of the lens, as seen in the insets of Fig. 3. However, there is a trade-off between this effect and the "level" of transformation, since for bigger values of y_0, those regions are reduced but the lens is flattened less, having a smaller focal line.

The bed of nails technology is chosen to implement the lens. The unit cell is depicted in Fig. 4 and consists of a perfect electric conductor (PEC) cylinder centered within the cell. There is a dielectric of $n = 3.271$, which corresponds to a commercial Rogers RT/duroid

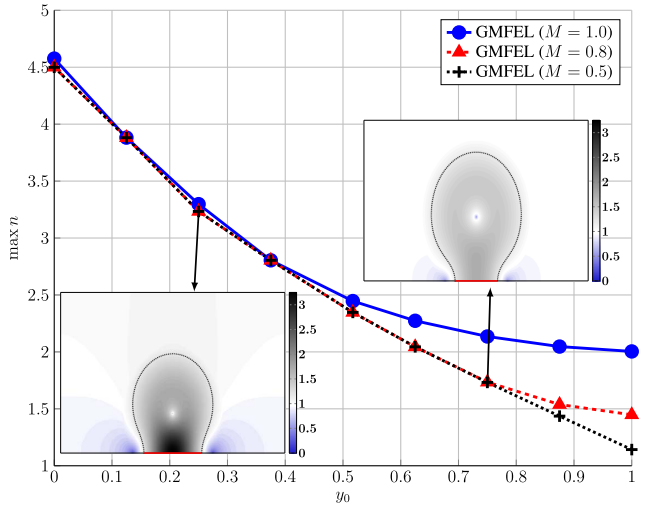

Fig. 3. Maximum value of the refractive index versus lens shift for three different lenses. The insets correspond to the GMFEL with $M = 0.8$ and the dotted contour to $n = 1.2$. The focal lines are shown with red solid lines in the insets.

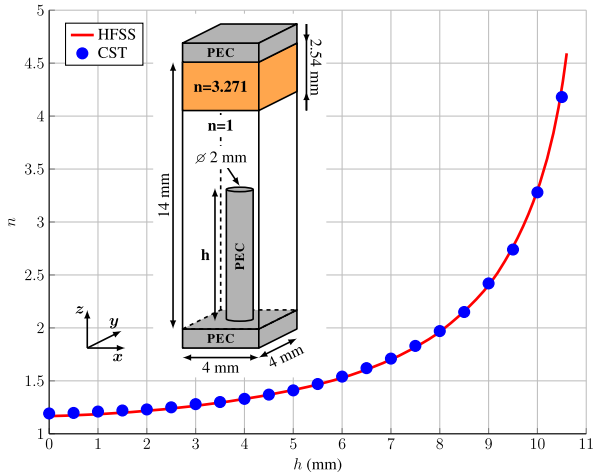

Fig. 4. Design curve using the bed of nails unit cell at 6 GHz.

6010.2LM. This new unit cell based on the bed of nails allows us to achieve higher values of refractive index as a function of the height of the metallic cylinder pin, thanks to the dielectric substrate placed on top of the cell. The values shown for the unit cell geometry in Fig. 4 were chosen after several parametric studies to obtain a suitable unit cell with only one design parameter. In particular, for low values of the periodicity and large values of the substrate and unit cell height, the design curve is less steep around the higher values of h. Additionally, by reducing the periodicity and increasing the cylinder diameter, the unit cell is less dispersive in frequency.

The design curve in Fig. 4 was obtained simulating the unit cell assuming local periodicity (i.e., embedding the unit cell in an infinite array comprised of the same unit cell) and computing its dispersion diagram for several values of h. By interpolating the data at the desired frequency, the refractive index as a function of h was obtained. Since the curves involved are smooth, the interpolation produces accurate data.

The minimum value of n in Fig. 4 is 1.167, so to use only one design curve, all refraction indices below such value have to be approximated by the minimum value achievable. In this case, we chose 1.18, which corresponds to $h = 0.97$ mm.

For the GMFEL with $M = 0.8$ and $y_0 = 0.25$, the refractive index maximum value is 3.23. Although it is achievable by the design curve, there is an additional strategy to reduce the maximum value. As done for the minimum value, the maximum refractive index can be saturated to a certain value, although in this case, it is an approximation to reduce the maximum value of n (as in contrast with the variation of y_0). If the saturation value is not far from the real maximum, the behavior of the lens will barely change. For the selected lens, we have chosen a saturation value of $n = 3.16$, although lower values are still possible without affecting excessively the behavior of the lens and avoiding the dispersive region of the design curve.

Figure 5 shows the implemented GMFEL using the bed of nails. It was generated after scaling the normalized transformed lens by 5λ at 6 GHz. It consists of 15251 cylinders and its dimensions are 0.6 m × 0.4 m. It is fed by a coaxial wire matched to 50Ω and placed in one side of the

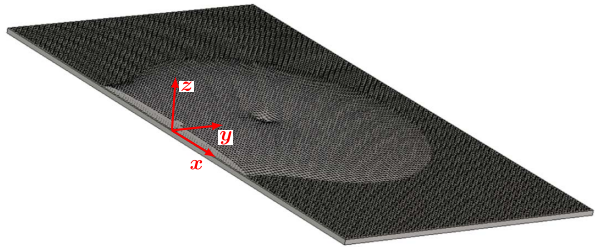

Fig. 5. CST implementation of the GMFEL with $M = 0.8$ and $y_0 = 0.25$ using the bed of nails technology. For clarity, the top PEC cover and dielectric have been removed.

lens at the location of the straight focal line. Open boundary conditions are enforced on the sides of the structure.

Simulation results for the GMFEL are shown in Figs. 6, 7. On the one hand, Fig. 6 presents the normalized electric field $\hat{z}$ component at two different planes at the design frequency (6 GHz). It can be clearly seen how the lens splits the power source into two points as it was expected. On the other hand, Fig. 7 shows the electric field in the same plane, but at two different frequencies, 5 and 5.5 GHz. For frequencies outside the range of 5 to 6 GHz, the lens does not work properly for several reasons, mainly the frequency dispersion of the unit cell for higher frequencies and the small size of the overall lens for lower ones. Notwithstanding, for this particular example, the GMFEL operates from 5 to 6 GHz, hence, having a total bandwidth of approximately 18% with a central frequency of 5.5 GHz.

In conclusion, we have applied transformation optics to improve dielectric lenses. First, because of the nature of the transformation, there is an effect of space compression which results in smaller sub-unity refractive index regions. This reduces the negative impact of approximating those regions with $n = 1$ to avoid materials with high losses and poor bandwidth. However, the

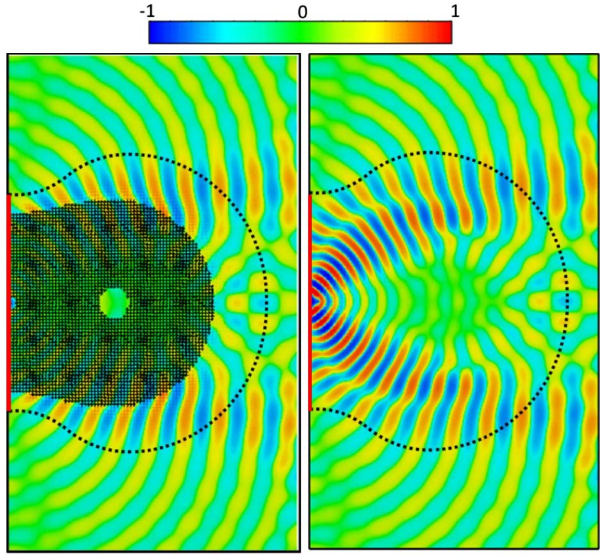

Fig. 6. Simulated GMFEL at 6 GHz corresponding to that of Fig. 5. Normalized electric field in the planes at 6 mm (left) and 12 mm (right) from the ground plane. The dotted contour corresponds to min $n = 1.18$. The focal line is shown in red solid line.

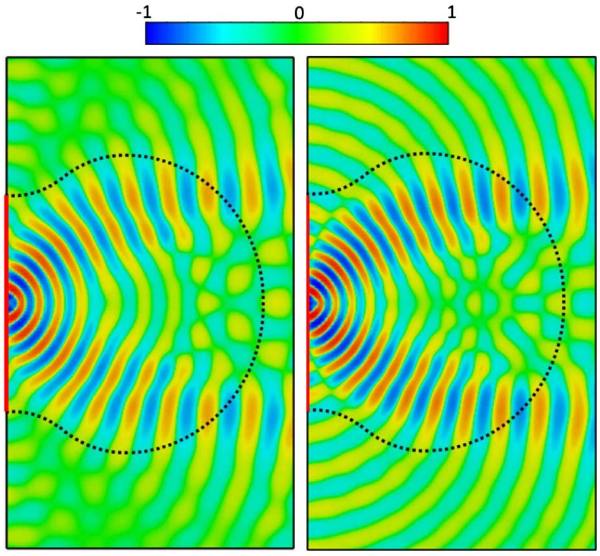

Fig. 7. Simulated GMFEL at 5 GHz (left) and 5.5 GHz (right) corresponding to that of Fig. 5. Normalized electric field in the plane at 12 mm from the ground plane. The dotted contour corresponds to min $n = 1.18$. The focal line is shown in red solid line.

transformation increases the maximum value of the refractive index, which is hard to obtain on cheap 2D technologies. Here, we presented a technique which can control this maximum value by reducing the space compression. However, there is a trade-off between the desired maximum value of refractive index and the length of the flattened focal line. These improvements were applied to the design of a GMFEL working as a power splitter. The bed of nails technology was employed, and the lens was generated and simulated with a 3D full-wave simulator obtaining a good performance. The techniques described in this Letter can be applied to other lenses and extended to implementations in other technologies. In particular, the bandwidth could be significantly improved by choosing an implementation with fully dielectric materials [18].

The authors would like to thank Dr. José Luis Vázquez Roy for his help in preparing the CST model of the lens. The participation of Daniel Rodríguez Prado in this work was supported by Gobierno del Principado de Asturias, under grant BP12-063.

References

1. U. Leonhardt, Science **312**, 1777 (2006).
2. J. B. Pendry, D. Schurig, and D. R. Smith, Science **312**, 1780 (2006).
3. D.-H. Kwon and D. H. Werner, IEEE Antennas Propag. Mag. **52**, 24 (2010).
4. K. Yao, X. Jiang, and H. Chen, New J. Phys. **14**, 023011 (2012).
5. D.-H. Kwon and D. H. Werner, New J. Phys. **10**, 115023 (2008).
6. O. Quevedo-Teruel, W. Tang, and Y. Hao, Opt. Lett. **37**, 4850 (2012).
7. F. Kong, B.-I. Wu, J. A. Kong, J. Huangfu, S. Xi, and H. Chen, Appl. Phys. Lett. **91**, 253509 (2007).
8. M. Rahm, S. A. Cummer, D. Schurig, J. B. Pendry, and D. R. Smith, Phys. Rev. Lett. **100**, 063903 (2008).
9. D. A. Roberts, M. Rahm, J. B. Pendry, and D. R. Smith, Appl. Phys. Lett. **93**, 251111 (2008).
10. C. D. Emiroglu and D.-H. Kwon, Appl. Phys. Lett. **107**, 084502 (2010).
11. A. Greenleaf, Y. Kurylev, M. Lassas, and G. Uhlmann, Phys. Rev. Lett. **99**, 183901 (2007).
12. D. Schurig, J. J. Mock, B. J. Justice, S. A. Cummer, J. B. Pendry, A. F. Starr, and D. R. Smith, Science **314**, 977 (2006).
13. W. X. Jiang, S. Ge, C. Luo, and T. J. Cui, Appl. Phys. Lett. **103**, 214104 (2013).
14. J. Li and J. B. Pendry, Phys. Rev. Lett. **101**, 203901 (2008).
15. S. A. R. Horsley, I. R. Hooper, R. C. Mitchell-Thomas, and O. Quevedo-Teruel, Sci. Rep. **4**, 4876 (2014).
16. N. Kundtz and D. R. Smith, Nat. Mater. **9**, 129 (2009).
17. D. Schurig, New J. Phys. **10**, 115034 (2008).
18. O. Quevedo-Teruel, W. Tang, R. C. Mitchell-Thomas, A. Dyke, H. Dyke, L. Zhang, S. Haq, and Y. Hao, Sci. Rep. **3**, 1903 (2013).